# We are IntechOpen,
# the world's leading publisher of
# Open Access books
# Built by scientists, for scientists

## 4,800
Open access books available

## 122,000
International authors and editors

## 135M
Downloads

Our authors are among the

## 154
Countries delivered to

## TOP 1%
most cited scientists

## 12.2%
Contributors from top 500 universities

CLARIVATE ANALYTICS

**BOOK
CITATION
INDEX**

INDEXED

**WEB OF SCIENCE**™

Selection of our books indexed in the Book Citation Index
in Web of Science™ Core Collection (BKCI)

# Interested in publishing with us?
# Contact book.department@intechopen.com

Numbers displayed above are based on latest data collected.
For more information visit www.intechopen.com

# Modification of Mackinawite with L-Cysteine: Synthesis, Characterization, and Implications to Mercury Immobilization in Sediment

Marcia R. M. Chaves[1], Kalliat T. Valsaraj[2], Ronald D. DeLaune[3],
Robert P. Gambrell[3] and Pedro M. Buchler[1]
*[1]Department of Chemical Engineering, University of Sao Paulo; Sao Paulo,*
*[2]Department of Chemical Engineering,*
*Louisiana State University, Baton Rouge, Louisiana,*
*[3]Department of Oceanography and Coastal Sciences,*
*Louisiana State University, Baton Rouge, Louisiana,*
*[1]Brazil*
*[2,3]USA*

## 1. Introduction

Environmental remediation of mercury contaminated sediment includes the inhibition or minimization of mercury methylation. Mackinawite (FeS) is an excellent material that inhibits mercury methylation (Liu et al, 2009). Effective remediation of sediment contaminated with mercury is essential in minimizing the contamination of fish and shellfish and, consequently, the human exposure to methyl mercury. In-situ capping (ISC) is one of the remediation methods that have been found to reduce the mercury transport from sediment to the overlying water. It consists of placing a proper layer of isolating material between the layers of contaminated sediment and overlying water (Palermo, 1998; Liu et al., 2007). This method is attractive due to the reduction in mobility and availability of the contaminant, and requires fewer infrastructures associated with handling, dewatering, treatment and disposal. Mackinawite was reported as an effective isolating material for use as a sediment cap (Liu et al, 2009).

Although pure mackinawite can immobilize mercury, it has a low stability when exposed to oxidized conditions (Burton et al, 2009; Liu et al, 2008; Wolthers et al, 2005). Under field conditions, the capping material has to be in contact with the oxigenated water column during the capping building. This process can oxidize the mackinawite, making this material unable to reacting with the contaminant. Therefore, is important to make the FeS more resistant to oxidation. To obtain stable mackinawite, we proposed to modify its surface using L-cysteine as an organic ligand, considering ferredoxin as a model. Ferredoxins are proteins that have an inorganic active core constituent of $Fe_2S_2$ or $Fe_4S_4$ bonded to L-cysteine groups. This core participates in electron-transfer, contributing to important biological functions such as respiration and photosynthesis (Fontecave and Ollagnier-de-Choudens,

2008). Piuille et al (1995) reported that the enzyme pyruvate-ferrodoxin oxyreductase was stable in $O_2$ (atmospheric air) and the L-cysteine groups seemed to provide the oxidation stability.

Some investigators have tested iron sulfide oxidation at environmental pH ranges (Burton et al, 2009; Bourdoiseau et al, 2008). Most of the literature is related to the oxidation of reduced iron sulfide compounds such as pyrite, troilite, and pyrrhotite under acidic conditions, for solving acid mine drainage issues (Moses et al, 2003). Mackinawite is considered a precursor to other iron-sulfides ($FeS_2$, $Fe_{1-x}S$, $Fe_{1+x}S$, $Fe_3S_4$), and should follow the same pattern of oxidation, occurring via intermediate polysulfide species, resulting in FeOOH and elemental $S^0$ or iron sulfate. Mackinawite oxidation can occur in biotic or abiotic conditions, but is not microbially mediated (Burton et al, 2009). In attempting to improve the oxidation resistance of pyrite, Zhang et al (2003) reported the suppression of pyrite oxidation by about 90%, through the polymerization of diacetylene groups in the lipid tails, producing a cross-linked layer on the mineral surface. Along the same lines, Belzile et al (1997) used a series of coating agents (acetyl acetone, humic acids, amonium lignosulfonates, oxalic acid and sodium silicate) to increase oxidation inhibition above 40%.

Our current study on anoxic sediment contaminated with mercury is to investigate the capability of mackinawite modified with L-cysteine to sequestrate mercury. It involves the effects of L-cysteine on mackinawite structure, oxidation stability, mercury uptake capacity, and inhibition of mercury methylation capacity. In this chapter, we present the synthesis and characterization of mackinawite modified with L-cysteine, the effect of this modification on the structure and oxidation stability of mackinawite, and its implication to mercury immobilization in contaminated sediment using capping technology.

## 2. Synthesis of modified mackinawite

Synthetic mackinawite was prepared from deoxygenated solutions of $(NH_4)_2FeSO_4 \cdot 6 H_2O$ (Mohr's salt; Sigma-Aldrich), and $Na_2S \cdot 9 H_2O$ (Acros Chemicals), using the method described by Liu et al (2008). The experiments were conducted under $N_2$, using a glove box, at room temperature (25°C), and all solutions were previously deoxygenated by purging with $N_2$ (ultra-pure) for 30 minutes.

The unmodified mackinawite (in this work is designed as FeS) was prepared by addition of 100 ml Mohr's salt (0.4 mol/l) to 100 mL of $Na_2S \cdot 9 H_2O$ (0.4 mol/l) in a three-necked flask, which was magnetically stirred for 15 minutes. The suspension was filtered using a 0.45μm membrane filter in a vacuum filtration system. The solid was placed in a HDPE centrifuge tube, $N_2$ was added to filled the empty space, the tube was tightly closed, placed into a vacuum-sealed bag, and stored in a freezer. After being frozen, the solid was removed from the freezer and returned to the reaction flask with 200 ml of water (HPLC grade) previously deoxygenated, stirred for 15 minutes and filtered. This procedure was repeated twice, and the solid was dried under a $N_2$ flow, and stored in 1.5 ml vials, preserved in a vacuum-sealed bag, until be used.

The modified mackinawite (in this work is designed as FeS-Cys) was prepared following the same procedure, except that 2.0 g of L-cysteine was dissolved in the Mohr's salt solution before reaction with the sodium sulfide solution. Although the reaction between Mohr's salt and sodium sulfide was effective, the gravimetric yield was 75%, due to solid losses during the filtration and drying process.

## 3. Mackinawite characterization

The characterization was performed by determination of mackinawite composition; crystallinity; specific surface area and porosity; morphology; oxidation resistance; and mercury uptake capacity. These characteristics were obtained using the techniques, instruments, and procedures as described following.

The chemical composition of the solids was determined by a Perkin Elmer 2400 CHNS Elemental Analyzer, and evaluated by FTIR (Nicolet 6700 FTIR), EDS (Jeol 840A), and XPS (Kratos AXIS 165 XPS/Electron Spectroscopy, with X-ray source of Al Kα (1253,6 eV), hybrid mode, 15kV of accelerating voltage,10 mA of current).

The crystallinity of the solids was obtained using a Bruker/Siemens D5000 automated powder X-ray diffractometer with CuKα. The data were collected in the interval from 2 to 70 degrees 2θ at a rate of 0.02 degrees per 2 seconds. The results were interpreted using the JADE software V6.1.

The SEM images and EDS spectra were obtained from samples coated with gold, using a Scanning Electron Microprobe (JEOL 840A) with 15 kV of accelerating voltage. TEM images were obtained from samples deposited on 200# Cu - Lacey carbon-coated discs, through the High Resolution Transmission Electron Microscope operated at 200 kV of accelerating voltage.

The specific surface area was measured following the multipoint $N_2$-BET adsorption method, using a QuantaChrome 500 instrument. The sample was transferred to the bulb tube of the instrument under a $N_2$ flow inside a glove box, sealed with Parafilm®, and transferred rapidly to the work station where it was degassed at room temperature overnight.

The oxidation experiments were carried out in a 250 mL three-necked flask, open to the atmosphere. The flask was placed in a water bath on a stirrer plate. In the neck of the flask were placed pH, $E_H$ and dissolved oxygen (DO) sensors. Water (250 mL HPLC grade) was added to the flask; the pH was controlled with additions of 0.1 M NaOH and/or HCl (trace metal grade) solutions. Mackinawite (0.5 g) was added to the water and stirred during the experiment.

The Ross Ultra combination pH sensor (ORION 8156BNUWP), with external automatic temperature compensation (ATC) probe, was calibrated before each measurement using commercial 4 and 7 pH buffer solutions, connected to pH/mV/°C meter (Oakton pH 510 series). The Eh sensor, a platinum sure-flow combination Redox-ORP type (Orion 89678BNWP), was calibrated using ORP standard solution (Orion 967901) at the same temperature of the experiment, connected to a Cole Parmer pH/mV/°C meter, giving direct Eh measurement. The dissolved oxygen was determined using a Mettler Toledo InLab® 605 sensor, with internal ATC probe, connected to Mettler Toledo SevenGo™ Pro SG6 DO meter, which was calibrated following the manual instructions, using oxygen-saturated water.

The experiments were conducted under both short and long time scales. Short time-scale (5 hours) experiments were evaluated at pH (4 to 8) and temperature (25°C to 45°C). Long time-scale experiments were performed at pH 6 and 25°C for 24 hours. Immediately at the end of each experiment, the solid was filtered using a 0.45μm Pall GN Metricel® mixed cellulose membrane filter, in a vacuum filtration system, dried under $N_2$ flow, and stored in 1.5 mL vials with $N_2$ to avoid posterior solids oxidation, sealed with parafilm®, and preserved in a vacuum-sealed bag.

The solids were evaluated using FTIR, obtained through powder direct analysis (Nicolet 6700 FTIR) collected by accumulation of 36 scans, 4 cm$^{-1}$ resolution, and using air as background. The crystallinity of the solids was obtained using a Bruker/Siemens D5000, as described early.

### 3.1 Chemical composition

*EDS Analysis*

The chemical composition was evaluated through energy dispersive spectroscopy (EDS) obtained on a scanning electron microscope (SEM). Figure 1 shows the spectra of samples of mackinawite, unmodified (FeS) and modified with L-cysteine (FeS-Cys). The presence of oxygen was observed in the unmodified mackinawite, but not in the sample modified with cysteine. This indicates a possible partial oxidation of the sample of unmodified mackinawite, and also some resistance to further oxidation of modified mackinawite.
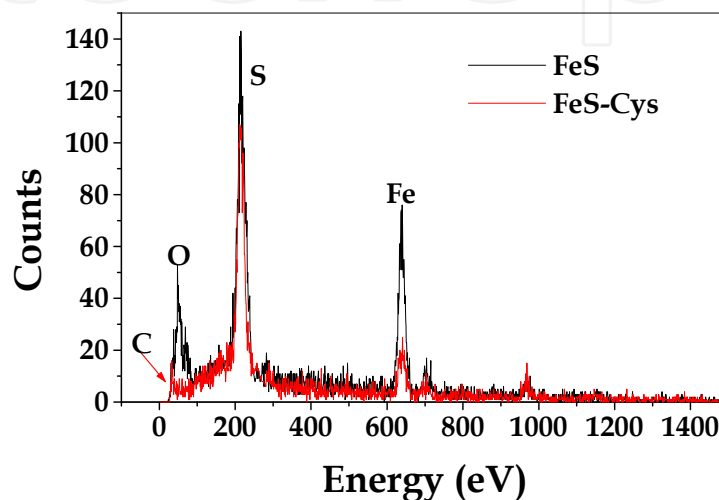


Fig. 1. Spectra of EDS of the mackinawites studied.

*FTIR Analysis*

The chemical composition was also evaluated through FTIR of the samples. The iron sulfides do not present clear absorption bands at lower wavenumber, in the infrared spectrum. Although it is not possible to distinguish the types of vibration between the atoms of iron and sulfur present in mackinawite, was possible to judge which bands are due to the presence of FeS, and which bands are characteristic of L-cysteine. In support of this evaluation, spectrum was obtained of Mohr's salt solution containing L-cysteine dissolved under the same conditions used in the preparation of modified mackinawite. The interaction between iron and L-cysteine may occur through interaction of iron-oxygen, iron-sulfur or iron-nitrogen, depending on the pH of the system.

The pH below 5 of the iron-cysteine solution facilitated the protonation of the cysteine. In this case the iron preferentially binds to the sulfur displaying a spectrum similar to mackinawite. The amount of cysteine was very lower than the iron; thus, the complex resulted was formed by attachment of one cysteine per atom of iron. From figure 2, it can be observed that the solution of iron and L-cysteine (Fe-Cys) showed bands characteristic of asymmetric stretching of carboxylate $(C\overset{\cdots}{-}O)_2$ at 1638 cm$^{-1}$ typical of amino acid, a weak band at 1451 cm$^{-1}$ characteristic of ammonium ion $NH_4^+$, and another at 1096 cm$^{-1}$ indicating the presence of sulfate $(SO_4^{2-})$ constituents of Mohr's salt. A broad band, centered in the region of 3300 cm$^{-1}$, comprises the vibration spectrum of the water in the solution superimposed on the band in 3340 cm$^{-1}$, relative to the N-H stretching in protonated amine

$(NH_3^+)$ of L-cysteine. The absence of the features of the connection with H-S at 2551 cm$^{-1}$, shows that iron is linked to the sulfur. We observed that mackinawite modified with cysteine showed an infrared spectrum almost identical to the original mackinawite, differing only by the presence of a broad band of low intensity, centered at 1583 cm$^{-1}$, assigned to the presence of carboxylate $(C\overline{\phantom{x}}O)_2$. The bands of low intensity in the region of 2200 cm$^{-1}$ to 1900 cm$^{-1}$ are attributed to the vibration of the Fe-S bond.
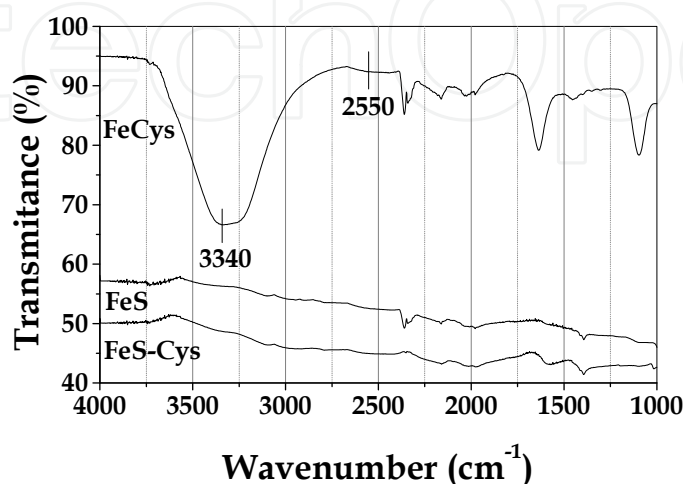


Fig. 2. FTIR of the iron-cysteine complex (FeCys), unmodified (FeS) and modified (FeS-Cys) mackinawite.

*XPS Analysis*

The X-ray photoelectron spectroscopy (XPS) is a characterization technique used to evaluate the surface of the sample. For mackinawite is particularly very useful because it can identify the presence of oxidation products on the surface of the sample, and the oxidation state of elements involved.

The survey spectra of modified and unmodified mackinawite indicated the presence of the elements C, O, Fe and S. The carbon is a ubiquitous contaminant, being found in all samples. Nevertheless, its presence results in a well-defined spectrum for modified mackinawite (Fig. 3a).

The spectrum consisted of two broad bands, which were decomposed using the software Origin 8.1 for Gaussian peaks. The identified peaks are characteristic of cysteine at 284.5 eV referring to the C-C bond, at 285.5 eV assigned to C-OH and C-N bonds. The peak at 288.4 eV and characteristic of the presence of C=O, found in both the cysteine as the adsorbed $CO_2$ from the air.

The XPS spectra of Fe $2p_{3/2}$ of the unmodified mackinawite (Fig. 3b) and mackinawite modified with cisteine (Fig. 3c) showed a broad band, result of combination of severals peaks, characteristic of the weathered surface of mackinawite. This corrosion was atributted to the exposure of the samples to ambient atmosphere during the sample preparation prior to insertion in the evacuated chamber of the XPS equipment.

The spectrum of unmodified mackinawite showed peaks at 707.9, 709.8 and 711.6, characteristic of Fe (II)-S, Fe (III)-S and Fe (III)-O bonds. For modified mackinawite, the peaks were identified at 707.7, 709.0 and 711.2, characteristic of Fe (II)-S, Fe (II)-O and Fe (III)-O. The presence of these peaks reveals a surface composed by mackinawite and oxy (hydroxy) of iron, such as goethite or lepidocrocite FeOOH.
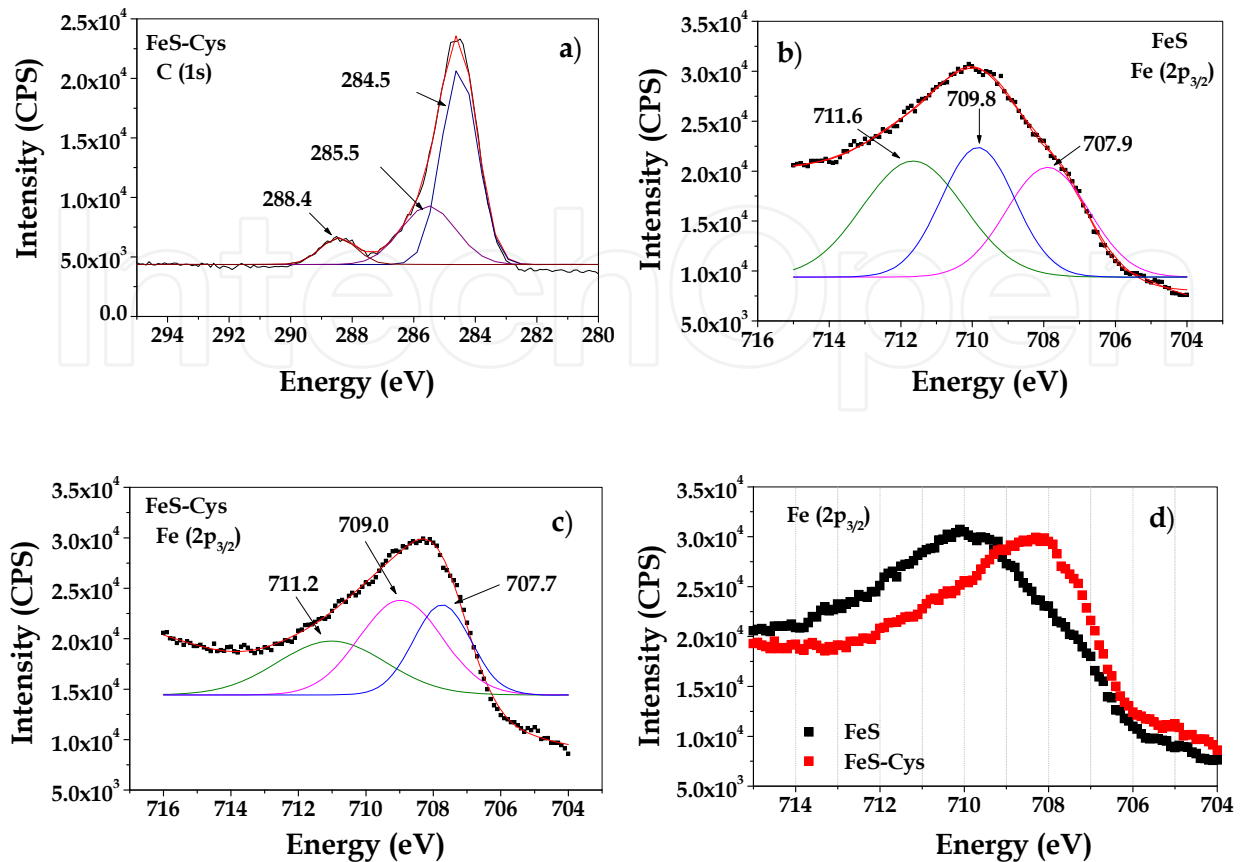
Fig. 3. XPS spectra of C (1s) a) FeS-Cys and Fe ( $2p_{3/2}$): b) FeS; c) FeS-Cys; d) merge of the Fe ($2p_{3/2)}$ curves. Errors for energy ± 0.3 eV.

By merging the curves into one graph, it can be observed that the spectrum presented by unmodified mackinawite is a result of greater contribution of oxidation products of its surface; modified mackinawite presented a relatively less weathered surface (Fig. 3d). This demonstrates the efficiency of cysteine to increase the oxidation resistance of mackinawite.

Similar to iron, the bands resulting from the sulfur 2p spectrum was decomposed, obtaining the peaks related to mackinawite and products of oxidation (Fig. 4a and 4b).

The peaks of unmodifed mackinawite were identified at 160.1 eV and 161.4 eV characteristics of ($S^{2-}$), 162.4 eV characteristic of ($S_2^{2-}$), 163.6 eV characteristic of ($S_n^{2-}$), 164.1 characteristic of ($S^0$), and a broad band centered at 169.0 eV attributed the presence of ($SO_4^2$). It is important to note the presence of polysulfides ($S_n^{2-}$) and elemental sulfur ($S^0$), typical for the oxidation of the surface mackinawite. The presence of sulfate is attributed more to the inefficient removal by mackinawite washing during the synthesis process, than the oxidation process. These results are in agreement with those obtained by other researchers (Nesbitt and Muir (1994); Behra et al (2001), Boursiquot et al, 2001; Mullet et al, 2001).

For modified mackinawite the identified peaks were centered at 160.3 and 161.2 eV characteristic of ($S^{2-}$), 161.8 eV characteristic of ($S_2^{2-}$), 163.0 eV characteristic of ($S_n^{2-}$), and 164.5 characteristic of ($S^0$).

The peak at 168.1 eV, attributed to sulfate ($SO_4^{2-}$) adsorbed, is well-defined with lower energy than that presented by unmodified mackinawite. This could be a result of the

adsorption of sulfate on cysteine, probably through hydrogen bonds between the hydroxyl and oxygen of the sulfate, with the amine and the carboxylate groups of the cysteine. Thus it made the sulfate removal more difficult, explaining the greater contribution in the spectrum. The results showed that the cysteine influences the oxidation process, since the modified mackinawite presented the sulfur 2p spectrum with greater contribution of the peaks characteristic of sulfide, and lower peak intensity of the polysulfide groups. For unmodified mackinawite, the formation of the spectrum of sulfur showed higher contribution of groups $S_2^{2-}$, polysulfides and elemental sulfur, ie, products of oxidation on its surface.
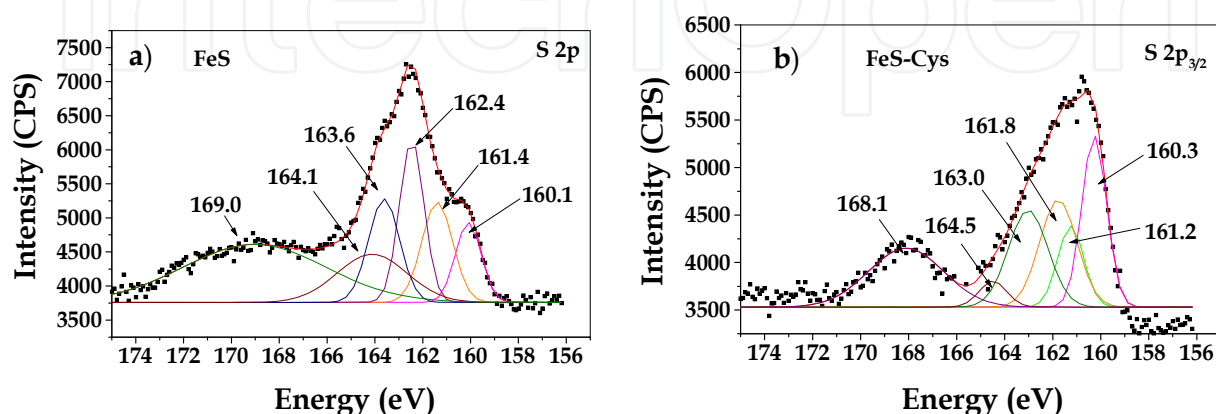


Fig. 4. XPS spectra of S 2p: a) FeS and b) FeS-Cys – Errors for energy ± 0.3 eV.

The XPS spectra of O 1s for both mackinawites are shown in the figures 5a and 5b. For unmodified mackinawite we identified the peaks at 529.4 eV attributed to species ($O^{2-}$), 531.6 eV attributed to the presence of hydroxyl ($OH^-$) present in iron hydroxide, the peaks at 533.0 eV attributed to adsorbed water molecule, and 534.2 eV attributed to the adsorbed ($CO_2$) from the air. For the modified mackinawite these peaks were identified at 529.3 eV, 530.7 eV, and 532.3 eV. The peak characteristic $CO_2$ adsorption was not present, and the intensity of the peak for adsorbed water was much lower than that reported in unmodified mackinawite, confirming the higher hydrophobic character of its surface, caused by the presence of cysteine.
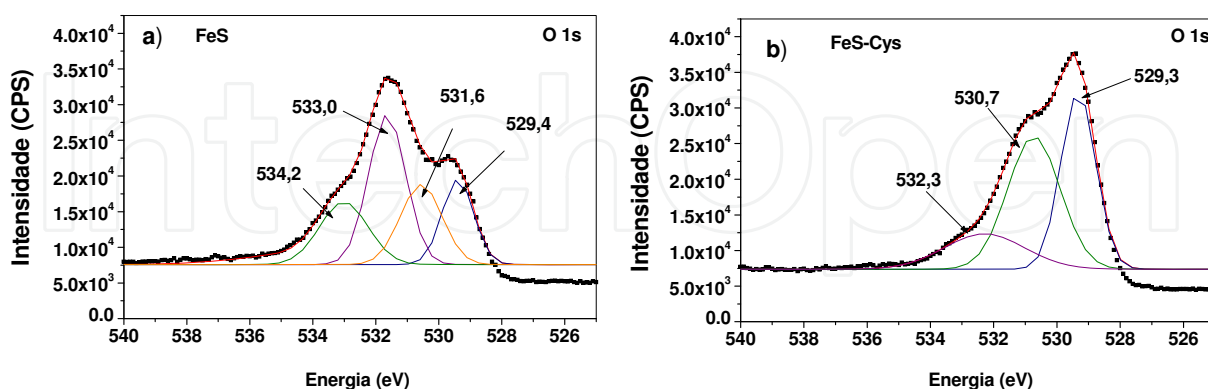


Fig. 5. XPS spectra of O 1s: a) FeS; b) FeS-Cys. Errors for energy ± 0.3 eV.

*Elemental (CHNS) Analysis*

Using elemental analysis (CHNS) and ICP-OES analysis to determine iron content, the chemical composition of unmodified mackinawite was determined as $FeS_{0.86}$. Sweeney and Kaplan (1973) also found that FeS has a composition of $FeS_{0.87-0.92}$. For modified

mackinawite, the carbon content is due to the amount of L-cysteine in the sample. As L-cysteine contains a sulfur atom in its molecule, the quantity of sulfur was subtracted from the total, resulting in the amount of sulfur corresponding to mackinawite (Equation 1).

$$S_{mackinawite} = S_{total} - S_{cysteine} \tag{1}$$

Considering the mass of carbon in the sample being equal to 0.6 g corresponding to L-cysteine, and each molecule of L-cysteine has 3 carbons and a sulfur atom, the amount of cysteine and hence of sulfur was determined to be 16.7 mmol (or 2 g). This amount is in line with the amount of cysteine added during the preparation of modified mackinawite (2.00 g), meaning that all the cysteine was reacted. Thus, the chemical composition of mackinawite modified with L-cysteine was determined as $FeS_{0.735}.Cys_{0.0133}$. The contents of each element are presented in table 1.

| Sample | C (% wt) | H (% wt) | N (% wt) | S (% wt) | Fe[a] (% wt) |
|---|---|---|---|---|---|
| FeS | nd | nd | nd | 32.1 | 67.9 |
| FeS-Cys | 0.6 | 2.1 | 1.2 | 28.9 | 67.2 |

[a] Determined by ICP_OES.

Table 1. Chemical analysis of unmodified (FeS) and modified (FeS-Cys) mackinawite.

### 3.2 Crystalline structure

X-ray diffraction analysis by the powder method confirmed the nano-crystalline structure of mackinawite. Figure 6 presents the XRPD pattern for the samples. There were low intensity peaks, characteristic of compounds with low crystallinity and/or nano-size of particles. The addition of L-cysteine to mackinawite modified the X-ray diffraction patterns. The main change is the increased intensity of the peak attributed to the (001) spacing with a small lower angle displacement of the peak. The change in chemical composition and increased (001) spacing indicate that L-cysteine reacts with the iron, when mixed during the synthesis, remains within the structure of mackinawite, occupying the spaces between the layers. This results in the observed lattice expansion.
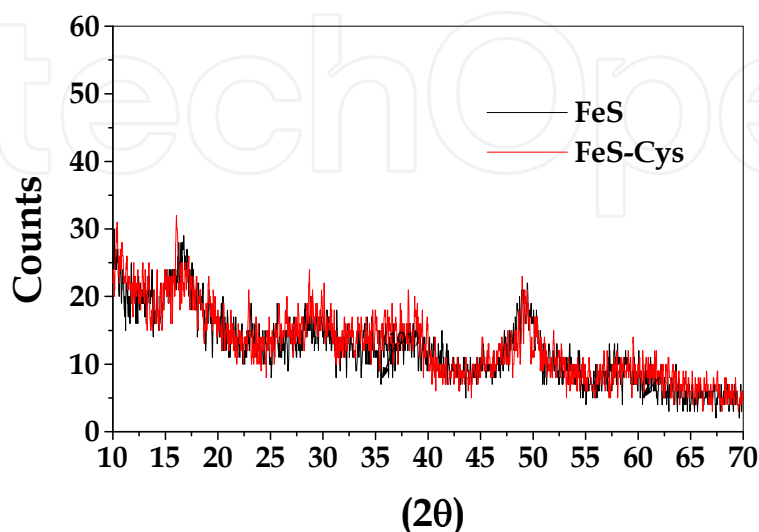


Fig. 6. XRPD pattern of FeS and FeS-Cys

Using the length and angle between the atoms, it was possible to calculate the length of the cysteine molecule, as approximately 0.432 nm (Ayyaar and Srinivasan, 1965). The lattice spacing for the mackinawite is 0.529 nm. This is large enough for the L-cysteine molecule to occupy and expand the lattice. This is aided by the electrostatic repulsion between the charges in the cysteine and on the surface of mackinawite.

The X-ray diffraction pattern of disordered mackinawite is not well-defined. However, it was possible to determine the diffraction of the characteristic peak of the plane (001) for unmodified and modified mackinawite – see Table 2.

|  | FeS[a] | FeS-Cys[a] | FeS-ref[b] | FeS[c] |
|---|---|---|---|---|
| hkl | d (Å) | d (Å) | d (Å) | D (Å) |
| 001 | 5.2913 | 5.5187 | 5.196 | 5.0328 |

[a] Synthetic disordered mackinawite aged for 3 h (this study)
[b] Synthetic mackinawite original - aged for 3 days (JEONG et al, 2008)
[c] Crystallized mackinawite (LENNIE et al, 1995 )

Table 2. XRPD parameter for synthetic mackinawite

### 3.3 Particle size and morphology

The particle size, and morphology of the solids was evaluated using a Nitrogen adsorption /desorption isotherm (BET), Scanning Electron Microscopy (SEM), and Transmission Electron Microscopy (TEM).

The nitrogen adsorption isotherms (BET) for mackinawite are shown in figure 7. The mackinawite exhibited typical adsorption curves (type III), but with a characteristic H3 type hysteresis. The isotherm of type III is unusual, and is exhibited by materials with low interaction with the adsorbate ($N_2$). The adsorption-desorption hysteresis is indicative of the type of pores on the surface of a solid. The type H3, where desorption occurs along the whole $P/P_0$ curve, results from clusters of particles of the lamellar type giving rise to the cleft-like
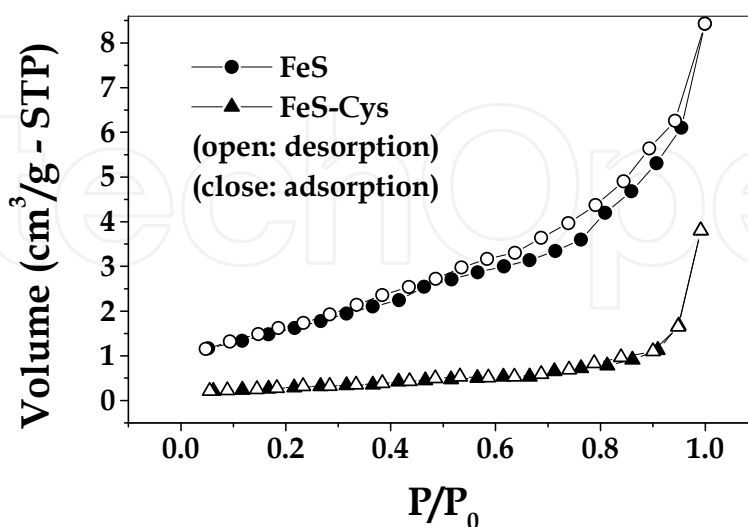


Fig. 7. $N_2$ adsorption/desorption isotherms of the unmodified mackinawite (FeS) and modified mackinawite (FeS-Cys). Average pore diameter and total pore volume: FeS 8.74 nm; $1.30 \times 10^{-2}$ $cm^3/g$ - FeS-Cys 23.09 nm; $0.59 \times 10^{-2}$ $cm^3/g$.

pores (Sing, 1985). This feature confirms the layered structure of mackinawite prepared. This characteristic is important in metal ion adsorption from the liquid medium. The values of average diameter and total pore volume of the mackinawite are shown in figure 7.

Results show that L-cysteine increases the average pore diameter, but decreases the total pore volume. The specific surface area was determined by $N_2$ adsorption/desorption technique, using the BET equation; the values observed experimentally are shown in table 3. Mackinawite is a nanosized material, the specific surface area determined by BET is underestimated, due the nitrogen does not cover properly all surface area, result of porous blocked by cysteine. Thus, it is useful just to make a comparison, and determine the effect of cysteine on the mackinawite surface. The experimental result of the unmodified mackinawite is in agreement with values described in the literature, ranging from 4.7 to 80 $m^2/g$. The effect of L-cysteine on the microstructure reduces significantly the specific surface area, and thus could influence the adsorption capacity of the modified mackinawite.

The SEM images present the shape of the clusters of unmodified and modified mackinawite (Fig. 8). The original mackinawite had clusters of particles mean spherical in shape, while modified mackinawite showed more elongated larger clusters. The effect of L-cysteine on the morphology of mackinawite can be explained based on the attachment of L-cysteine during the synthesis, between the layers of mackinawite. When L-cysteine is mixed with Mohr's salt, the complex $[HO_2CCH(NH_2)CH_2S]Fe^+$ is formed in solution. The reaction of this solution with sodium sulfate solution, results in a solid containing a portion of the carbon

| Material | Specific surface area ($m^2/g$) | Particle diameter (nm) | Reference |
|----------|---------|---------|-----------|
| FeS | 5.97 | 5.0[a] | This work |
| FeS-Cys | 1.02 | 5.0[a] | This work |
| FeS | 7.0 | 210[b] | Taylor et al. (1979) |
| FeS | 36.5 | 40[b] | Rickard (1997) |
| FeS | 80 | 18[b] | Widler (2002) |

[a] determined by TEM analysis; [b] calculated using BET specific surface area.

Table 3. Specific surface area and particle diameter for synthetic mackinawite
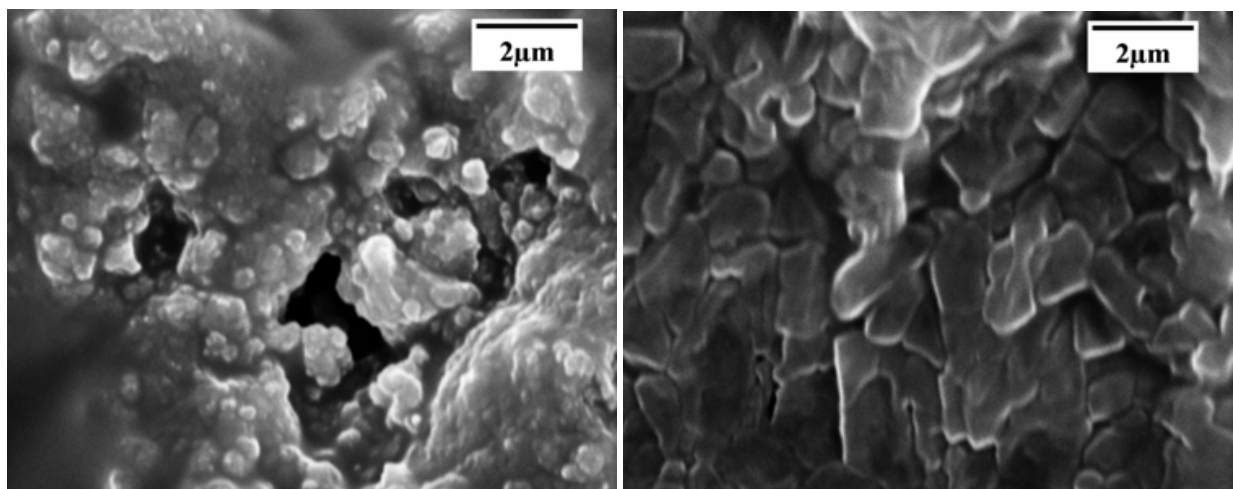


Fig. 8. Scanning Electron Microscopy: a) unmodified mackinawite; b) modified mackinawite. (10,000 x magnification).

Modification of Mackinawite with L-Cysteine:
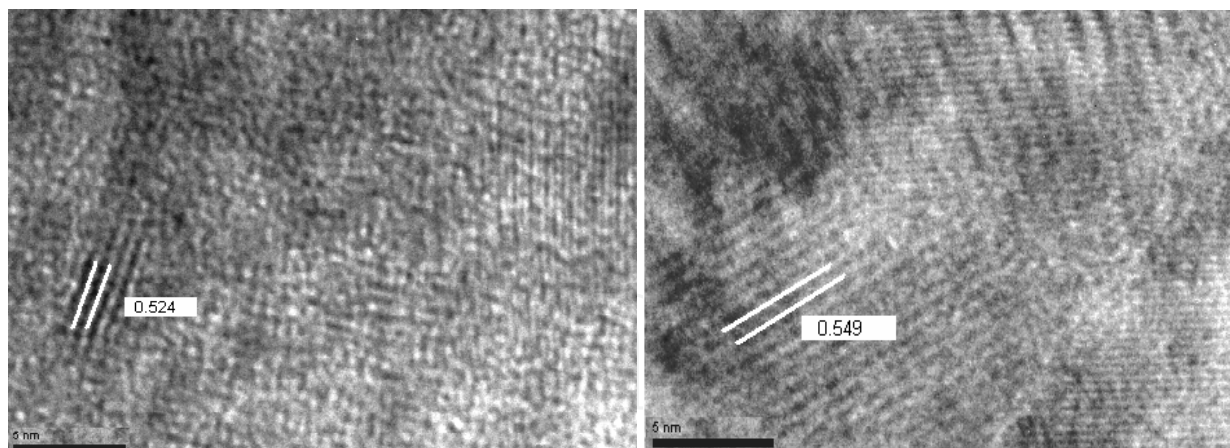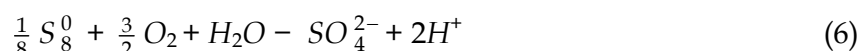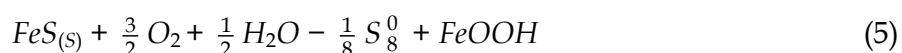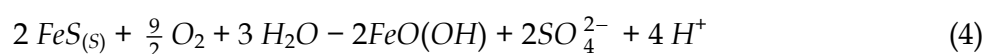Synthesis, Characterization, and Implications to Mercury Immobilization in Sediment

323

Fig. 9. High Resolution Transmission Electron Microscopy of a) unmodified mackinawite; b) modified mackinawite.

chain of L-cysteine, on the surface. The interaction of amine and carboxylate groups with atoms of iron in the adjacent layer, should limit the configuration to a lamellar shape. Thus, the presence of L-cysteine between the sheets of the FeS, forces the clusters to form plates.

The unmodified and modified mackinawite analyzed by TEM (Fig. 9a and 9b) presented particles in average diameter of 5 nm. The samples were poor crystallized, but some crystals allowed to identify the space between the layers ($d_{001}$) as being 5.24 Å and 5.49 Å for unmodified and modified mackinawite, respectively. These values are close to those observed using XRPD analysis, and support the information that the cysteine is located between the layers in the mackinawite structure, resulting in the lattice expansion.

### 3.4 Effect of L-cysteine on mackinawite oxidation

*Mackinawite oxidation – Short time-scale experiments*

The solubility of mackinawite (FeS) in water with pH lower than the pH of point of zero charge ($pH_{pzc}$=7.5), is a pH-dependent reaction (equation 2). Above $pH_{pzc}$, the solubility is a pH-independent reaction (equation 3), and the aqueous species are neutral and consist in $Fe_nS_n$ or clusters with Fe:S ratio of 1(Rickard, 2006). The oxidative dissolution of FeS is a process that can be described by serveral reactions (equations 4-6), being the pH a important parameter.

$$FeS_{(S)} + H_2O + H^+ - HS^- + Fe^{2+} \tag{2}$$

$$nFeS_{(S)} - Fe_nS_{n\,(aq)} \tag{3}$$

$$2\,FeS_{(S)} + \tfrac{9}{2}\,O_2 + 3\,H_2O - 2FeO(OH) + 2SO_4^{2-} + 4\,H^+ \tag{4}$$

$$FeS_{(S)} + \tfrac{3}{2}\,O_2 + \tfrac{1}{2}\,H_2O - \tfrac{1}{8}\,S_8^0 + FeOOH \tag{5}$$

$$\tfrac{1}{8}\,S_8^0 + \tfrac{3}{2}\,O_2 + H_2O - SO_4^{2-} + 2H^+ \tag{6}$$

When mackinawite was added to water, a fast increase of pH to a maximum occurred within the first minute, which decreased slowly to no more than one unit below the

maximum (Fig. 10). This behavior indicates the existence of two processes, viz., the fast protonation of the surface, followed by mackinawite surface oxidation. The protonation of mackinawite surface is favored due to the high content of sulfur atoms.
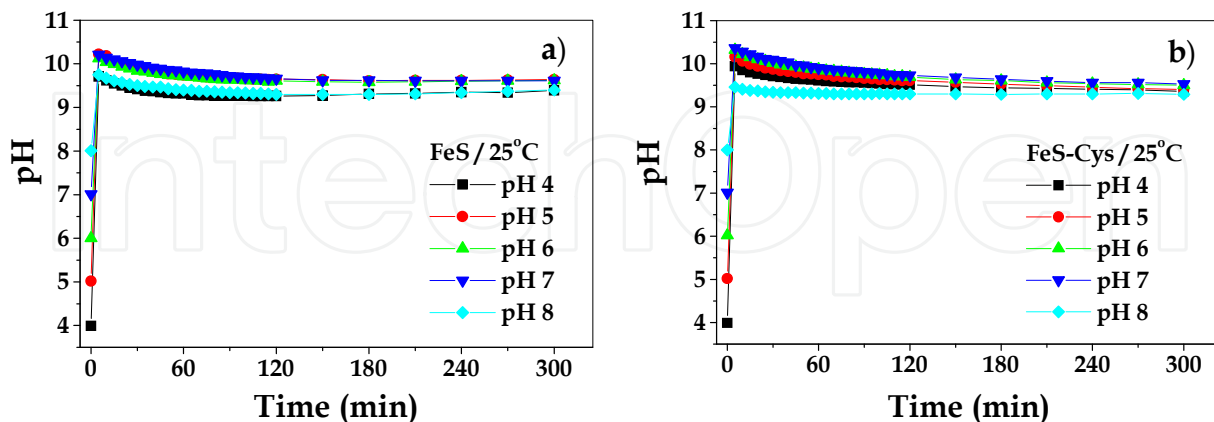


Fig. 10. pH solution during the mackinawite oxidation process (short time).

Mackinawite when added to water (2 g/l) produced a strongly reduced environment within the first minute of contact, resulting from surface protonation and sorption of dissolved oxygen. The redox potential increased gradually during the following 5 hours, attributed to gradual increase of amount of oxidized species in solution.

The redox characteristics of unmodified mackinawite were not sensibly affected by initial pH, whereas that of the modified mackinawite showed sensible to initial pH (Fig. 11). The Eh was more negative at initial pH values between 4 and 7 indicating progressive resistance to oxidation.

The modified mackinawite showed the same trend of Eh behavior presented by unmodified mackinawite in initial pH 4 to 7; however, the Eh was more sensible to initial pH than the unmodified mackinawite. It can be explained by the variable charge surface of cysteine, and its protonation/deprotonation with pH change.

The Eh of solutions containing FeS-Cys was lower than that of FeS under the same conditions throughout the experiments, indicating that cysteine increased the mackinawite oxidation resistance, as showed earlier by XPS analysis. This can be observed through the XRPD (Fig. 12) and FTIR (Fig 13) analyses of the solids obtained after 5 hours of experiment.

The effect of initial pH is more visible to the peak at 14 (2θ), characteristic of lepidrocrocite. The intensity of this peak decrease wiht increasing pH range 4-6, and increase with decreasing the pH range 7-8. This behavior indicates that the oxidation process decreased until pH 6, increasing to higher pHs. This is in agreement with the mackinawite surface chemistry (Mullet et al, 2002).

There is a lower intensity of the peaks caracteristic of sulfur (S) and lepdocrocite (L), and the highest band intensity characteristic of mackinawite (M) in the XRPD pattern of the FeS-Cys in relation to the XRPD pattern of the FeS.

The FTIR spectra of FeS oxidized at different initial pHs showed bands at 668, 743, 795 and 885 cm$^{-1}$, and 3127 cm$^{-1}$, associated with the stretch modes and δOH vOH of lepidocrocite, respectively. A band of low intensity at 3730 cm$^{-1}$ and due to the stretching of the OH free connection, similar to the silanol on the surface of silica. Elemental sulfur (S$^0$) has no stretch modes in the spectrum. The bands at 1200, 1120 and 996 cm$^{-1}$ can be attributed to sulfate adsorbed on the surface of lepdocrocite. This is similar to sulfate adsorbed on goethite (Peak

Modification of Mackinawite with L-Cysteine:
Synthesis, Characterization, and Implications to Mercury Immobilization in Sediment
325

et al., 1999). The band expanded in 2000 and 2150 cm$^{-1}$ indicate the stretching of the Fe-S bound in mackinawite.
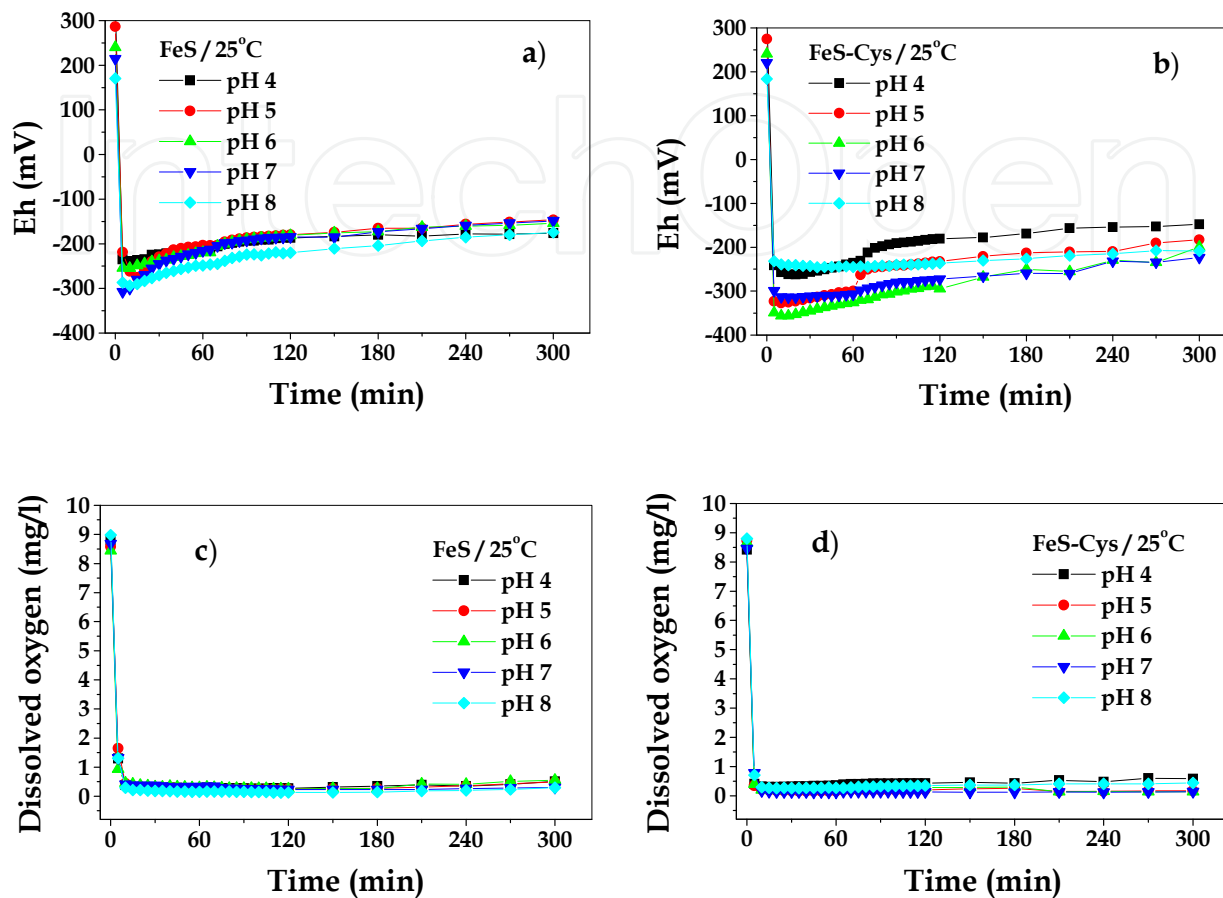


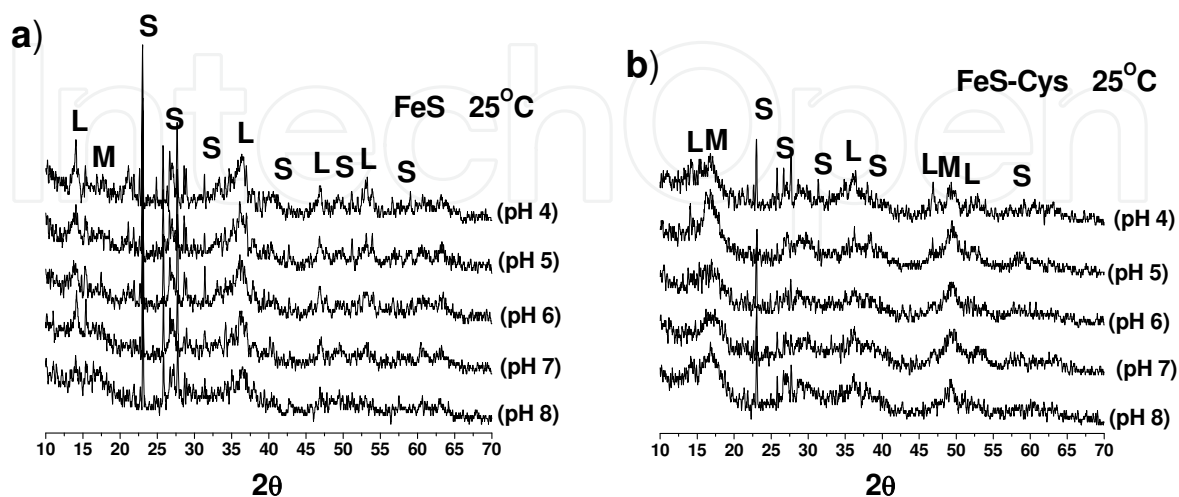Fig. 11. Eh and DO of solution during the oxidation of mackinanwite (short time).



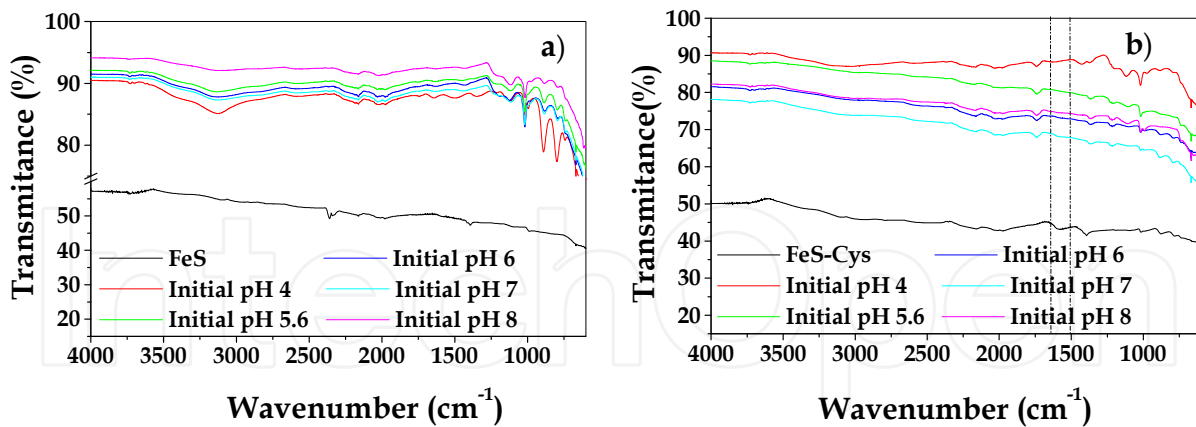Fig. 12. XRPD pattern of the solids after oxidation experiments (short time). (L) lepidocrocite; (S) sulfur; (M) mackinawite.

Fig. 13. FTIR spectra of a) unmodified and b) modified mackinawite after oxidation processes (short time)

The FeS-Cys showed the characteristic bands of the OH vibration of lepdocrocite (668, 739, 794, 883, and 3128 cm⁻¹), the low intensity band in the 3730 cm⁻¹ is attributed to stretching of free OH, and bands associated to the presence of sulfate (1200, 1120 and 996 cm⁻¹).

Similar to the XRPD, the FTIR spectrum of the FeS shows visible difference, with greater intensity of the peaks associated with the presence of sulfate and lepdocrocite, in relation to FeS-Cys, indicating greater susceptibility to oxidation.

*Effect of the temperature on the mackinawite oxidation*

The effect of temperature on the mackinawite oxidation was also evaluated (Fig. 14). It was observed that an increase in temperature inhibits the oxidation process. The oxidation reaction is dependent on the dissolved oxygen in water, which decreases at higher temperatures. We observed a difference in the Eh of the solution of FeS and FeS-Cys at 25°C and 35°C, but in 45°C all the samples showed the same behavior, due the critical concentration of dissolved oxygen have limited the oxidation process.

By comparison, the FeS showed a higher degree of oxidation than the FeS-Cys at different temperatures, observed through the peak of characteristic X-ray diffraction of the oxidation products (lepidocrocite and sulfur) (Fig. 15).
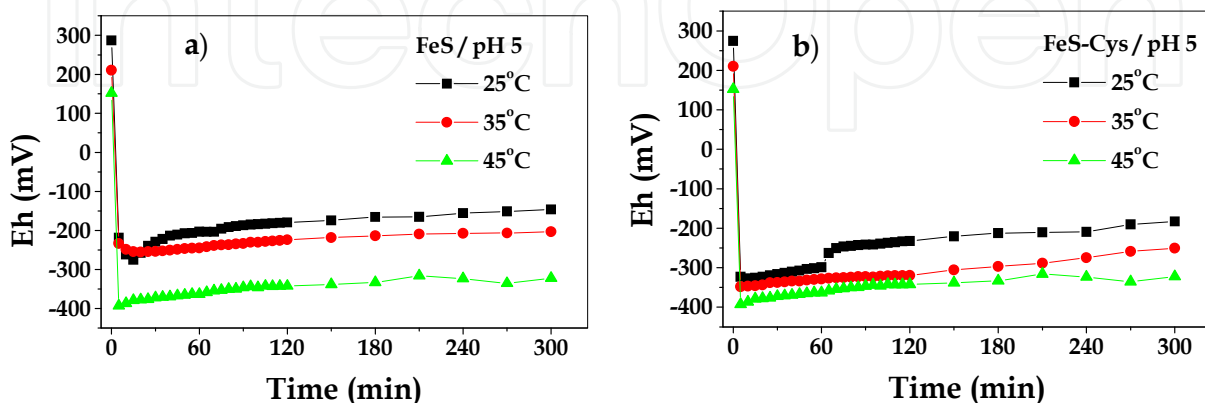


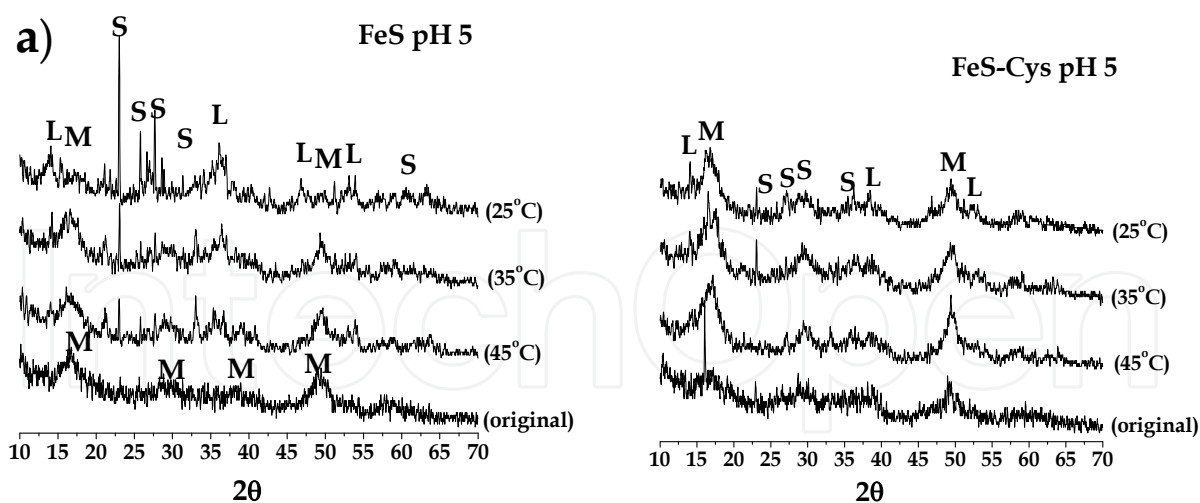Fig. 14. Effect of temperature on the mackinawite oxidation process.

Fig. 15. XRPD pattern of the solids after oxidation experiments in diferent temperatures (short time).

*Mackinawite oxidation – Long time-scale experiments*

The unmodified mackinawite (FeS) has low resistance to oxidation (Liu et al, 2008, Wolters et al, 2005). In preliminary analysis (not shown), we observed that FeS oxidized in less than 24 hours. Thus, this period was selected to evaluate the oxidation process in experiments of long time scale.

The redox potential of the solutions followed the same pattern as that described for the short time experiments. After strong initial reduction, the Eh increased during the next 24 hours.

The FeS-Cys showed lower Eh throughout the experiment, compared to the FeS, indicating increased stability towards oxidation (Fig. 16a). In the graph of Eh vs. time, it is possible to observe two distinct regions (a and b). The boundary between these regions was defined as a function of change of slope of the curve, denoting a change in the kinetics of the process. The point that occured this process was accompanied by color change of suspension. For FeS, after nine hours of agitation in the experimental conditions described, the suspension changed from black to red very quickly, attributed to the oxidation of iron (II) of the mackinawite to iron (III). The modified mackinawite showed the same pattern, except that the region was extended up to 14 hours.

The time required for the onset of advanced oxidation was considered as a parameter to evaluate the oxidation resistance, since the experiments were performed under the same conditions, varying only the type of solid. Thus, the increase in 5 hours observed for the modified mackinawite represented an increase of 55% in relation to unmodified mackinawite.

The results are in agreement with the model proposed by Chiriţă et al (2008) for the oxidative dissolution of a mixture of 4M pyrrhotite and troilite. According to this model and the experimental results, the mechanism of oxidation of mackinawite is based on the process of protonation and surface oxidation (phase a), and the collapse of the surface with the fast oxidation of the bulk solid (phase b).

The mackinawite surface is protonated upon contact with the water (equation 7). Protonated groups react with adsorbed oxygen, making the surface-rich in sulfide groups (equation 8). Sulfide groups ($\equiv S_m^{2-}$) prevent the diffusion of oxygen to the bulk solid, resulting in lower oxidation rate, which was called inhibition oxidation phase (phase a). The decrease in pH, observed experimentally supports this information.

The iron released into the solution reacts with oxygen and is oxidized to iron oxide-hydroxide, which precipitates as lepdocrocite (equation 9).

$$\equiv FeSH^0 + H^+ \rightarrow \equiv FeSH_2^+ \tag{7}$$

please, send me this eq with second proof form **in mathtype** (8)

$$Fe^{2+} + O_2 + H^+ \rightarrow FeO(OH) \tag{9}$$

The inhibition and fast oxidation of mackinawite also are characterized by the concentration of dissolved oxygen (Fig. 16c). When mackinawite (FeS and FeS-Cys) was added to water, the dissolved oxygen concentration decreased rapidly, making the system anoxic within five minutes. The system remained below 0.5 mg/l during 9 and 14 hours, respectively, for FeS and FeS-Cys. Then, the DO increased until the saturation value of approximately 7 mg/l. The amount of oxygen consumed in this process was determined using the Fick's law of diffusion, the diffusion coefficient of oxygen in water ($1.96 \times 10^{-5}$ cm²/s), the area of the reaction flask, and the gradient of concentration of oxygen, considering 1mm of the surface water (Table 4).

As shown in figure 16c the dissolved oxygen was continuously consumed during the inhibition phase. Chiriță and Descostes (2008) proposed that the impermeability of the oxidized surface layer is a function of the length and position of the polysulfide chains.
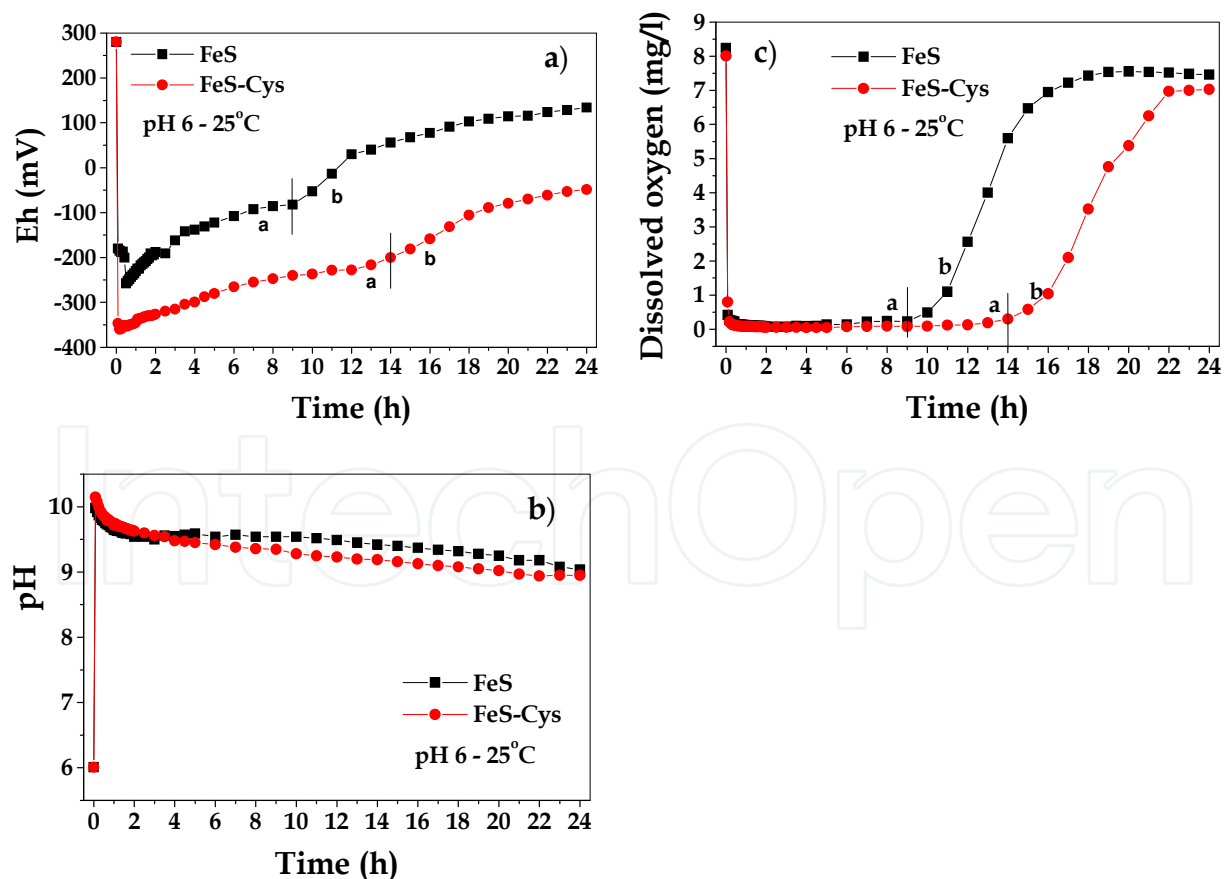


Fig. 16. Eh, pH and DO of the suspension during the oxidation process of mackinawite (long time).

| Phase | FeS Consummed $O_2$ (mol) | FeS-Cys Consummed $O_2$ (mol) |
|---|---|---|
| Initial adsorption + inhibition | 5.854 x$10^{-4}$ | 7.810 x$10^{-4}$ |
| Fast oxidation | 1.318 x$10^{-4}$ | 1.035 x$10^{-4}$ |

Table 4. Oxygen consummed during the mackinawite oxidation.

Short chains can easily undergo rearrangement in structures with close packing, reducing the mobility of the oxidant species. As the chains increase in size, it become more permeable, and the bulk solid oxidize faster.

The increase in polysulfide chains occurs through an oxidation process, catalyzed by proton, according to equation 10. Thus, the higher pH indicate the presence of long chains of polysulfide, with higher oxidant diffusion capacity. The lower $H^+$ concentration during the inhibition phase produced by unmodified mackinawite (Fig. 16b and Fig. 17) in comparison with modified mackinawite, indicates its lower oxidation resistence.

$$\equiv S_m^{2-} + \frac{1}{2} O_2 + 2H^+ \rightarrow \ \equiv S_n^{2-} + H_2O \tag{10}$$
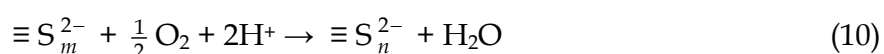
The end of the inhibition phase is the collapse of the surface layer of polysulfides, which facilitates the diffusion of oxygen, resulting in fast oxidation of the material (phase b). As cysteine does not polymerize, its presence on the modified mackinawite surface should result in small polysulfides chains. This promotes the increased of the oxidation resistance observed.

The mechanism of oxidation of iron sulfides (II) under acidic conditions involves the oxidation of Fe (II) to Fe (III). Researchers have proposed that iron (III) acts as the preferred oxidizing agent for sulfur, ie, the process of electron transfer from sulfur to iron (III) is easier in comparison to transfer to the oxygen (Chiriţă and Descostes, 2006; Burton et al, 2009; Kamei and Ohmoto, 2000; Bourdoiseau et al, 2008).

In this work, the FeS consumes less oxygen than the FeS-Cys. To explain the fact that FeS present higher oxidation and lower oxygen consumption, we propose that the polysulfide chains in this material grow through oxidation by Fe (III) (equation 11).

$$\equiv S_m^{2-} + Fe^{3+} \rightarrow \ \equiv S_n^{2-} + Fe^{2+} \tag{11}$$

This reaction is minimized in the system FeS-Cys, since part of the iron released is bound to cysteine through the formation of complexes $Fe(Cys)^+$. Thus, a larger amount of oxygen is consumed during the surface oxidation of modified mackinawite.

The concentration of protons as function of time is shown in Fig. 17. The concentration of $[H^+]$ is a result of several reactions that occur in suspension. Therefore, this parameter can only be used as a comparison between the two systems, since the experiments were executed under same conditions, being the cysteine the unique difference. The observations were supported by other analytical techniques results, such as the XRPD pattern.

The surface oxidation of sulfide groups ($\equiv S_m^{2-}$) (equation 8) produces protons, while the oxidation of iron sulfides and oxidation of the polysulfide groups ($\equiv S_n^{2-}$) (equations 9 and 10), consume protons.

Analyzing the concentration of $[H^+]$ in the oxidation process was observed that FeS-Cys releases more $[H^+]$ than FeS, attributed the formation of sulfide groups ($\equiv S_m^{2-}$) and the limited growth of polysulfide chains. This supports the assumption that the oxidation

resistance is due of the small polysulfide chains, which can rearrange, keeping the surface layer more impermeable to oxidation for longer time.
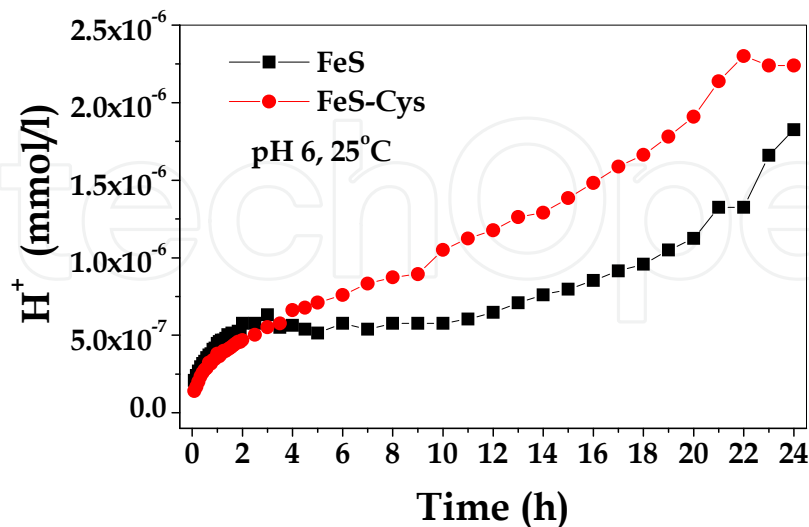


Fig. 17. [H+] concentration during the mackinawite oxidation process (long time), starting after pH maximum.

Mackinawite oxidation resulted in the formation of lepidocrocite and elemental sulfur, as early discussed for experiments of short time. This is in agreement with the features of the crystal structure of mackinawita since the lepidocrocite structure consists of layers of octahedra of iron oxide (III) joined by hydrogen bonding to hydroxyls. This also is in agreement with the oxidation product of the abiotic FeS (Burton et al, 2009).

After 24 hours, both mackinawites (FeS and FeS-Cys) had advanced oxidation states. The XRPD pattern of the solids before (1 and 3) and after (2 and 4) oxidation are shown in the figure 18.
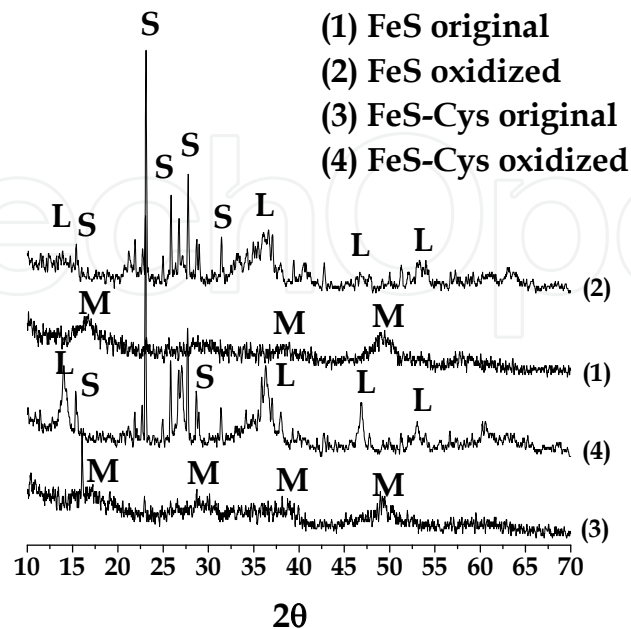


Fig. 18. XRPD pattern of the solids after 24h of oxidation process.

It is clear that the absence of the broad-band 16.5° (2θ) is characteristic of disordered mackinawite. The peaks of lepidocrocite formed by oxidation of FeS-Cys were better defined than for FeS, characteristic of higher crystallinity. This suggests that cysteine can control the microstructure during the formation of lepidocrocite.

### 3.5 Mercury uptake capacity

The mercury uptake experiments were conducted using 50 ml glass centrifuge tubes. A 5 mmol/l stock solution was prepared by dissolving of $HgCl_2$ (99.9995%, Alfa Aesar) in 32 mmol/l $HNO_3$ solution (trace metal grade, concentrate) in high pure water (HPLC grade). A Hg(II) 1 mmol/l solution was prepared by dilution of the stock solution, and purged with $N_2$ ultra high pure during 30 minutes; then, 0.4 g/l of the mackinawite was added into the solution, and magnetic stirred by a PTFE coated stirrer bar during 1, 5, 10, 20, 30, 60, and 90 minutes. After the desired time, the samples were filtered using a Whatmann seringe filter 0.45μm, being completed within 30 seconds after sampling. The 10 ml sample was preserved with addition of 20 μl of $HNO_3$ solution (trace metal grade, concentrate). The mercury content was determined using cold vapor method CVAAS (mercury Instruments, Lab Analyzer 254) based on EPA method # 7470 A.

Experiments to determine the mercury sequestration capacity of the studied mackinawites was carried through, using solution of $HgCl_2$ dissolved in high pure water. Results showed that unmodified and modified mackinawite is capable to uptake 99.99% and 99.94%, respectively, of mercury in solution within 30 minutes of contact (Fig. 19). It means that the modification with L-cysteine does not showed sensible influence on the mercury uptake; approximately 490 mg Hg/g mackinawite in medium concentration of 1mmol/l Hg (II) was observed, being an excellent material for mercury sequestration.
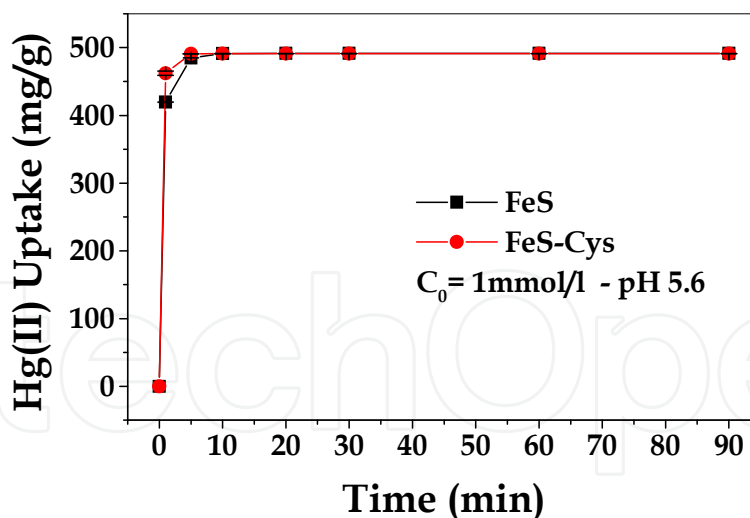


Fig. 19. Mercury uptake by unmodified (FeS) and modified (FeS-Cys) mackinawite.

### 4. Implications to mercury immobilization in contaminated sediment

The use of mackinawite as a reactive material in an active barrier system (ABS) associated with in-situ capping (ISC) will improve the mercury uptake in a contaminated sediment, since mercury does not have a large chemical affinity to silicate-based materials commonly used in ISC.

In spite of its excellent capability to immobilize mercury, one limitation characteristic to use of the mackinawite in ISC is due it easily be oxidized when applied as a reactive material to natural sediments. The modification of mackinawite, using the amino acid L-cysteine, increases its oxidation resistance, which can make possible the mackinawite aplication as ISC reactive material. The time to build a capping using mackinawite needs to be evaluated, for determine if the increase in the mackinawite oxidation resistance by cysteine is enough to its use.

Results from this study have shown that the modification of mackinawite occured using a simple experimental procedure, the efficiency of L-cysteine in retarding the mackinawite oxidation was 55%, and has a high mercury uptake capability, without sensible difference in comparison to the unmodified mackinawite. These are important features and therefore, modified mackinawite should be tested as a reactive capping material under laboratory conditions using mercury contaminated field sediments.

## 5. Acknowledgements

## 6. References

Ayyar, R. R., Srinivasan, R. (1965). Crystal structure of L (+) hydrochloride monohydrate. *Current Sc.* Vol. 34, No. 15, pp. 449-450.

Belzile, N., Maki, S., Chen, Y-W., and Goldsack, D. (1997). Inhibition of pyrite oxidation by surface treatment. *Sci. Total Environ.* Vol. 196, No. 2, pp. 177-186.

Behra, P. et al. (2001). XPS and XAS study of the sorption of Hg(II) onto pyrite. *Langmuir*, Vol. 17, pp. 3970-3979.

Bourdoiseau, J. A. et al. (2008). Characterization of mackinawite by Raman spectroscopy: effects of crystallization, drying and oxidation. *Corrosion Sci.* Vol. 50, pp. 3247-3255.

Boursiquot, S. et al (2001) The dry oxidation of tetragonal $FeS_{1-x}$ mackinawite. *Phys. Chem. Minerals* Vol. 28, pp. 600-611.

Burton, E. D. et al. (2009). Iron-monosulfide oxidation in natural sediments: resolving microbially mediated s transformations using xanes, electron microscopy, and selective extractions. *Environ. Sci. Technol.* Vol. 43, pp. 3128-3134.

Chiriţă, P., Descostes, M. (2006). Troilite oxidation by hydrogen peroxide. *J. Colloid Interface Sci.* Vol. 299, pp. 260-269.

Chiriţă, P. et al. (2008). Oxidation of FeS by oxygen-bearing acidic solutions. *J. Colloid Interface Sci.* Vol. 321, pp. 84-95.

Fontecave, M., and Ollagnier-de-Choudens, S. (2008). Iron–sulfur cluster biosynthesis in bacteria: Mechanisms of cluster assembly and transfer. *Arch. Biochem. Biophys.* Vol. 474, pp. 226-237.

Jeong, H. Y., et al. (2008) Characterization of synthetic nanocrystalline mackinawite: Crystal structure, particle size, and specific surface area. *Geochim. Cosmochim. Acta*, Vol. 72, pp. 493-505.

Kamei, G.; Ohmoto, H. (2000). The kinetics of reactions between pyrite and O2-bearing water revealed from in situ monitoring of DO, Eh and pH in a closed system. *Geochim. Cosmochim. Acta*,Vol. 64, pp. 2585-2601.

Lennie, A. R. et al. (1995). Synthesis and Rietveld crystal structure refinement of mackinawite tetragonal FeS. *Min. Mag.*, Vol. 59, pp. 677-683.

Liu, J. et al. (2007). Observations of mercury fate and transport beneath a sediment cap. *Land Contamination & Reclamation,* Vol. 15, pp. 401-411.

Liu, J. et al. (2008). Immobilization of aqueous Hg(II) by mackinawite (FeS). *J. Hazard. Mater.*, Vol. 157, pp. 432-440.

Liu, J. et al. (2009). Inhibition of Mercury Methylation by Iron Sulfides in an Anoxic Sediment. *Environ. Eng. Sci.*, Vol 26, pp. 833-840.

Moses, C. O. Nordstrom, D. K., Herman, J. S., and Mills, A. L. (1987). Aqueous pyrite oxidation by dissolved oxygen and by ferric iron. *Geochim. Cosmochim. Acta*, Vol. 51, pp. 1561-1571.

Mullet, M. et al. (2002) Surface chemistry and structural properties of mackinawite prepared by reaction of sulfide ions with metallic iron. *Geochim. Cosmochim. Acta* Vol. 66, pp. 829-836.

Nesbitt, H. W, Muir, I. J. (1994). X-ray phoelectron spectroscopic study of a pristine pyrite surface reacted with water vapour and air. *Geochim. Cosmochim. Acta* Vol. 58, ( 1994), pp. 4667-4679.

Palermo, M. R. (1998). Design considerations for in-situ capping of contaminated sediments. *Wat. Sci. Tech.* Vol. 37, ( 1998), pp. 315-321.

Peak, D.; Ford, R. D.; Sparks, D. L. (1999). An in situ ATR-FTIR investigation of sulfate bonding mechanisms on goethite. *J. Colloid Interface Sci.*, Vol. 218, pp. 289-299.

Pieulle, L., Guigliarelli, B., Asso, M., Dole, F., Bernadac, A., and Hatchikian C. E. (1995). Isolation and characterization of the pyruvate-ferredoxin oxidoreductase from the sulfate-reducing bacterium Desulfovibrio africanus. *Biochim. Biophys. Acta*, Vol. 1250, pp. 49-59.

Rickard, D. (1997). Kinetics of pyrite formation by the H2S oxidation of iron (II) monosulfide in aqueous solutions between 25 and 125°C: The rate equation. *Geochim. Cosmochim. Acta*, Vol. 61, pp. 115-134.

Rickard, D. (2006).The solubility of FeS. *Geochim. Cosmochim. Acta*, Vol. 70, pp. 5779-5789.

Sing, K. S. W. (1985) IUPAC: Reporting physisorption data for gas/solid systems with special reference to the determination of surface area and porosity (Recommendations 1984). *Pure appl. Chem.*, Vol. 57, pp. 603-619.

Sweeney, R. E., and Kaplan, I. R. (1973) Pyrite framboid formation, laboratory synthesis and marine sediments, Econ. Geol., Vol. 68, pp. 618-634.

Taylor, P., Rummery, T.E., and Owen, D.G. (1979). On the conversion of mackinawite and greigite. J. *Inorg. Nucl. Chem.*, Vol. 41, pp. 595-596.

Widler, A. M. (2002). The adsorption of gold (I) hydrosulphide complexes by iron sulphide surfaces. *Geochim. Cosmochim. Acta*, Vol. 66, pp. 383-402.

Wolthers, M., Charlet, L., van Der Linde, P. R., Rickard, D., and van Der Weijden, C. H. (2005) Surface chemistry of disordered mackinawite. *Geochim. Cosmochim. Acta*, Vol. 69, No. 14, pp. 3469-3481.

Zhang, X., Borda, M., Schoonen, M. A. A., and Strongin, D. R. (2003). Pyrite oxidation inhibition by a cross-linked lipid coating. *Geochem. Trans.* Vol. 4, No. 2, pp. 8-11.
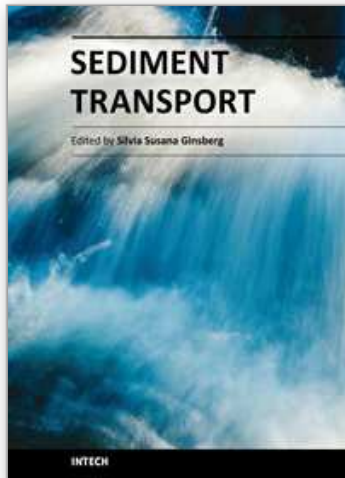
**Sediment Transport**

Edited by Dr. Silvia Susana Ginsberg

Sediment transport is a book that covers a wide variety of subject matters. It combines the personal and professional experience of the authors on solid particles transport and related problems, whose expertise is focused in aqueous systems and in laboratory flumes. This includes a series of chapters on hydrodynamics and their relationship with sediment transport and morphological development. The different contributions deal with issues such as the sediment transport modeling; sediment dynamics in stream confluence or river diversion, in meandering channels, at interconnected tidal channels system; changes in sediment transport under fine materials, cohesive materials and ice cover; environmental remediation of contaminated fine sediments. This is an invaluable interdisciplinary textbook and an important contribution to the sediment transport field. I strongly recommend this textbook to those in charge of conducting research on engineering issues or wishing to deal with equally important scientific problems.

# INTECH
open science | open minds